PAPER

Check for updates

Assessing the importance of nitric acid and ammonia for particle growth in the polluted boundary layer†

Ruby Marten, [a] Mao Xiao, [a] Mingyi Wang, [b] Weimeng Kong, [b] Xu-Cheng He, [cd] Dominik Stolzenburg, [ce] Joschka Pfeifer, [fg] Guillaume Marie, [g] Dongyu S. Wang, [a] Miriam Elser, [s] Andrea Baccarini, [ah] Chuan Ping Lee, [a] Antonio Amorim, [i] Rima Baalbaki, [c] David M. Bell, [a] Barbara Bertozzi, [j] Lucía Caudillo, [g] Lubna Dada, [a] Jonathan Duplissy, [ck] Henning Finkenzeller, [l] Martin Heinritzi, [g] Markus Lampimäki, [c] Katrianne Lehtipalo, [cd] Hanna E. Manninen, [f] Bernhard Mentler, [m] Antti Onnela, [f] Tuukka Petäjä, [c] Maxim Philippov, [n] Birte Rörup, [c] Wiebke Scholz, [m] Jiali Shen, [c] Yee Jun Tham, [c] António Tomé, [o] Andrea C. Wagner, [glp] Stefan K. Weber, [fg] Marcel Zauner-Wieczorek, [g] Joachim Curtius, [g] Markku Kulmala, [c] Rainer Volkamer, [l] Douglas R. Worsnop, [cq] Josef Dommen, [a] Richard C. Flagan, [b] Jasper Kirkby, [fg] Neil McPherson Donahue, [r] Houssni Lamkaddam,*[a] Urs Baltensperger[a] and Imad El Haddad *[a]

Aerosols formed and grown by gas-to-particle processes are a major contributor to smog and haze in megacities, despite the competition between growth and loss rates. Rapid growth rates from ammonium nitrate formation have the potential to sustain particle number in typical urban polluted conditions. This process requires supersaturation of gas-phase ammonia and nitric acid with respect to ammonium nitrate saturation ratios. Urban environments are inhomogeneous. In the troposphere, vertical mixing is fast, and aerosols may experience rapidly changing temperatures. In areas close to sources of pollution, gas-phase concentrations can also be highly variable. In this work we present results from nucleation experiments at −10 °C and 5 °C in the CLOUD chamber at CERN. We verify, using a kinetic model, how long supersaturation is likely to be sustained under urban conditions with temperature and concentration inhomogeneities, and the impact it may have on the particle size distribution. We show that rapid and strong temperature changes of 1 °C min^{-1} are needed to cause rapid growth of nanoparticles through ammonium nitrate formation. Furthermore, inhomogeneous emissions of ammonia in cities may also cause rapid growth of particles.

aLaboratory of Atmospheric Chemistry, Paul Scherrer Institute, 5232 Villigen, Switzerland. E-mail: houssni.lamkaddam@psi.ch; imad.el-haddad@psi.ch

bCalifornia Institute of Technology, Division of Chemistry and Chemical Engineering 210-41, Pasadena, CA 91125, USA

cInstitute for Atmospheric and Earth System Research/Physics, Faculty of Science, University of Helsinki, 00014 Helsinki, Finland

dFinnish Meteorological Institute, FI-00560 Helsinki, Finland

eInstitute for Materials Chemistry, TU Wien, 1060 Vienna, Austria

fCERN, CH-1211 Geneva, Switzerland

gInstitute for Atmospheric and Environmental Sciences, Goethe University Frankfurt, 60438 Frankfurt am Main, Germany

hAtmospheric Processes and Their Impact, École Polytechnique Fédérale de Lausanne, 1015 Lausanne, Switzerland

iCENTRA, FCUL, University of Lisbon, 1749-016 Lisbon, Portugal

jInstitute of Meteorology and Climate Research, Karlsruhe Institute of Technology, 76021 Karlsruhe, Germany

kHelsinki Institute of Physics (HIP)/Physics, Faculty of Science, University of Helsinki, 00014 Helsinki, Finland

iDepartment of Chemistry, CIRES, University of Colorado Boulder, 215 UCB, Boulder, 80309, CO, USA

mInstitute of Ion Physics and Applied Physics, University of Innsbruck, 6020 Innsbruck, Austria

nLebedev Physical Institute of the Russian Academy of Sciences, 119991, Leninsky prospekt, 53, Moscow, Russian Federation

oIDL-Universidade da Beira Interior, 6201-001 Covilhã, Portugal

pAerosol Physics Laboratory, Physics Unit, Tampere University, FI-33014 Tampere, Finland

qAerodyne Research, 01821 Billerica, MA, USA

rCenter for Atmospheric Particle Studies, Carnegie Mellon University, 1521 Pittsburgh, PA, USA

sEmpa, Swiss Federal Laboratories for Materials Science and Technology, Dübendorf, Switzerland

† Electronic supplementary information (ESI) available. See DOI: https://doi.org/10.1039/d3ea00001j

© 2024 The Author(s). Published by the Royal Society of Chemistry

Environ. Sci.: Atmos., 2024, **4**, 265–274 | **265**

Environmental significance

Urban aerosol pollution is detrimental to human health, and can affect local climate and visibility. Current understanding of new particle formation, survival, and growth in polluted environments is incomplete, ambient measurements suggest that either scavenging of small particles is overestimated, or there is a missing growth mechanism. Rapid growth from ammonium nitrate formation can cause an increase in particle number concentration in polluted conditions. Since supersaturated conditions are required, it is unclear how this growth might occur in ambient urban conditions. We illustrate, using an experimentally validated temperature sensitive kinetic model of ammonium nitrate growth, that inhomogeneities typical of polluted environments cause sufficient supersaturation for rapid growth of nanoparticles and a resulting increase in particle number concentration.

1 Introduction

Aerosols affect global and local climate by aerosol–radiation and aerosol–cloud interactions, where aerosol–cloud interactions are the larger forcing agent.[1] Aerosols must grow into the 50–100 nm diameter size range to be able to act as cloud condensation nuclei (CCN).[2] As well as acting as CCN, nucleation and growth of aerosols in urban environments can lead to persistent pollution, which is a leading cause of disability and death.[3,4] Therefore, it is important to understand key drivers of nucleation and growth.

Nucleation and growth in urban environments have been studied in depth through ambient measurements, chamber experiments, and models.[5–9] In polluted conditions, the high number of large particles act as a high coagulation sink (CoagS), which is a large loss term for small particles (<10 nm) as they have high Brownian diffusivity and so collisions with larger particles are more frequent.[2] In order for newly formed particles to escape scavenging by the CoagS, the growth rates need to outcompete the loss rates.[10] Aerosols grow from condensation of supersaturated vapours and ambient measurements suggest that growth rates in cities are only up to a few times greater than those in clean environments, while coagulation sink values are much higher. Due to this, newly formed particles are not expected to be able to grow to large sizes in typical urban conditions. Nevertheless, new particle formation events have often been observed, with particle formation rates up to hundreds of times higher than in clean environments.[11] Until recently there was no experimental evidence for an explanation of the persistence of high particle number concentrations sustained over a long time in the face of high loss processes. Wang *et al.* (2020)[12] introduced a new mechanism of ammonium nitrate formation, which rapidly grows particles as small as a few nanometres to much larger sizes.[12] Marten *et al.* (2022)[13] showed that this growth was high enough to grow small particles through the most critical size range (the "valley of death" from nucleation until approximately 10 nm) even in the presence of high condensation sinks, thus sustaining particle number concentrations. They also presented evidence that small particles are efficiently scavenged by larger particles and therefore over-estimating of loss rates is not the reason for the discrepancy in particle survival.

The mechanism of growth *via* ammonium nitrate formation is extremely sensitive to temperature, as temperature strongly affects the saturation concentrations and therefore growth rates. Urban environments are inhomogeneous. In the troposphere, mixing is relatively fast, especially vertical mixing, which involves a rapid change in temperature.[2,14] Furthermore,

there are many sources with highly variable emission rates which result in varying gas phase concentrations.[15] This may result in high supersaturation ratios of ammonia and nitric acid over particulate ammonium nitrate, which may rapidly grow nanoparticles. However, how long these supersaturations may be sustained for has not been quantified. Hence, the importance of ammonium nitrate on particle growth and survival remains unknown.

In this study we present results from the CLOUD experiment and modelled values of growth from ammonium nitrate at 5 °C and −10 °C, showing that the kinetic model is capable of replicating behaviour at different temperatures. Additionally, we use the kinetic model to assess how perturbations in temperature and concentration of NH_3 affect the growth of ammonium nitrate, and whether ammonium nitrate could be supersaturated in typical urban conditions on a timescale relevant to make significant changes to the existing particle size distribution.

2 Methods

2.1 CLOUD experiments

The experiments presented were undertaken in the CLOUD chamber at CERN in 2018. The CLOUD chamber is a 26.1 m^3 stainless steel nucleation chamber with controllable temperature, relative humidity, mixing speed, and irradiation.[16–18] Gas concentrations are controlled by a state of the art injection system. Experiments were performed at 5 °C and −10 °C, at 60% relative humidity, all experiments were conducted without use of the 3.5 GeV/*c* secondary pion beam (π beam) from the CERN proton synchrotron. In order to onset nucleation, condensable gases such as sulfuric acid (H_2SO_4), ammonia (NH_3), di-methyl amine, and organic oxidation products were generated. This was achieved *via* photolysis of ozone and/or HONO to generate OH radicals with UVA generated at 385 nm by a 400 W UVA LED saber and/or a 170 W quartz-clad high intensity Hg lamp. Rapid growth *via* ammonium nitrate formation was achieved by supersaturation of gas phase NH_3 and HNO_3, by injecting directly into the chamber, or producing HNO_3 *via* reaction of NO_2 and OH radicals. All precursor gases are in steady state when the experiments are started by the onset of photolysis and optimal mixing in the chamber. For further experimental details see Marten *et al.* (2022).[13]

2.2 CLOUD chamber model

A kinetic model illustrating growth from ammonium nitrate formation was developed and presented in Marten *et al.* (2022).[13] It was shown that the model could accurately replicate

results from CLOUD experiments at 5 °C. The model was revised to conditions at −10 °C. The main changes are a new Kelvin diameter fit from CLOUD experiments at −10 °C, and adjusting other parameters that are temperature dependent, such as the saturation concentration of ammonium nitrate (K_p),[19] the collision rate of particles, and the wall losses of particles.[20]

2.2.1 Kelvin diameter. The Kelvin diameter for ammonium nitrate at −10 °C was calculated by fitting the data from CLOUD experiments to eqn (1).

$$S_{AB,P} = 10(d_{K10}/d_{act}) \qquad (1)$$

where $S_{AB,P}$ is the saturation of ammonium nitrate, d_{K10} is the Kelvin diameter, and d_{act} is the activation diameter. The saturation concentration can be calculated from the mixing ratios of ammonia and nitric acid and the dissociation constant of ammonium nitrate. The Kelvin diameter is the diameter at which $S_{AB,P} = 10$, and the activation diameter is the minimum diameter at which ammonium nitrate can condense on particles. For more detailed information see the ESI† of Marten *et al.* 2022.[13]

2.2.2 Growth rates – N$_2$O$_5$. In 4 out of 10 experiments at −10 °C, growth *via* ammonium nitrate formation was not sufficient to explain the observed growth rates. For all experiments, we modelled the concentrations of N_2O_5, and show that this may potentially contribute to growth. Four experiments, which utilized ozone photolysis to produce OH, had higher ozone concentrations and therefore had higher concentrations of N_2O_5 *via* reaction of NO_3 radicals with NO_2. Six experiments with low O_3 concentration and negligible N_2O_5 utilised HONO photolysis to produce OH, as we intended to avoid NO_3 radical reactions with organics present (Table S1†). For these models, in order to calculate the N_2O_5 concentration, we used the Atchem online solver with inputs from the Master Chemical Mechanism (MCM)[21,22] for reaction rates, together with measured concentrations of O_3, NO, NO_2, SO_2, HONO, HNO_3, and organics present, photolysis rates, and loss rates of vapours from the CLOUD chamber. The process of heterogeneous uptake of N_2O_5, especially on nanoparticles, is uncertain. Therefore, for simplicity, we treated the calculated N_2O_5 concentration as additional HNO_3 for these 4 experiments, although we do not use these data points for fitting the Kelvin diameter of ammonium nitrate. N_2O_5 was also treated to have wall losses equivalent to those of sulphuric and nitric acid, concentrations where wall loss was not considered are also shown in Table S1.† Growth rates calculated without N_2O_5 parameterisation are shown in Fig. S1.†

2.3 Ambient model

The model was further adapted to model ambient conditions. The wall and dilution losses of the chamber were replaced with diffusion losses. Diffusion losses were calculated using equations from Seinfeld and Pandis (2006),[2] with literature deposition velocities for HNO_3, NH_3, and H_2SO_4.[2,23] The height of the boundary layer used was 1 km. The production values of HNO_3, NH_3, and H_2SO_4 were calculated such that in the absence of a condensation sink, the values were at steady state. These

calculations and examples of values used are shown in the ESI.† We also include a simulated condensation and coagulation sink (CondS = 0.005 s^{-1}) typical of moderately polluted urban air,[12] with an initial lognormal particle size distribution, which is centred at 200 nm. All model simulations are implied to have the same relative humidity of the experiments (60%). The effect of relative humidity is not covered in this model as it was not simulated in the CLOUD experiments and therefore would not have been experimentally validated. Nucleation rates (J_x) were calculated using a model based off of the general dynamic equation that is described in detail in Xiao *et al.* (2021).[2,11] Eqn (2) shows a simplified version of the equation, showing that loss rates (losses) are subtracted from the change in concentration of particles of a certain size x (N_x) over time (t). The units of J_x are particles per cm^3 per s.

$$J_x = \frac{dN_x}{dt} - \text{losses} \qquad (2)$$

Both the parameterization in Xiao *et al.* (2021) and the experiments presented in this paper were undertaken in the presence of galactic cosmic rays (*i.e.* with the clearing field of the CLOUD chamber off). However, we have not considered the effect of varying ionization level during vertical transport. For the "air parcel rising" experiments, the nucleation rates used for these models were input rates of 1.7 nm particles, they are temperature dependent and typical of 1×10^7 molecules per cm^3 H_2SO_4 with 3 ppbv NH_3 and no amines as seen in previous CLOUD experiments and ambient studies, presented in Xiao *et al.* 2021.[11,24,25] For the "concentration inhomogeneities" experiments, the nucleation rates were not constrained and kinetic nucleation rates were used, based on clusters of H_2SO_4 as in Marten *et al.* (2022).[13]

2.3.1 Air parcel rising. For experiments where we simulated an air parcel rising by a change in temperature, we constrained the temperature time-series to that of an increase and decrease in height. For these experiments, an average Kelvin diameter of the measurements at 10 °C and 5 °C was used for all temperatures. We also adjusted the temperature sensitive parameters as explained in the previous section. The temperature change used is 15 °C within 15 minutes as the air packet rises and falls.[12] Sensitivity tests were performed, varying the range and speed of the temperature change, the nucleation rate, and the initial temperature (Fig. S2–S5†).

2.3.2 Concentration inhomogeneities. In order to simulate inhomogeneities in the atmosphere, we used highly time-resolved ambient measurements. NH_3 was chosen rather than HNO_3 since the latter molecule is of secondary origin and therefore more homogeneously distributed than NH_3. Ambient time-series were reviewed to determine how often and how high increases in NH_3 concentration could be. This is heavily dependent on location, as spikes in NH_3 concentration are closely linked to traffic.[15] The time-series used is meant to simulate air parcels close to a point source of ammonia, for example near busy roads. We analysed time-series from two campaigns, the first was a mobile campaign in Zurich (Switzerland) in October 2013, the second a mobile and stationary

campaign in Tallinn and Tartu (Estonia) in March–April 2014.[15] For background NH_3 concentrations, we took the average over background stationary measurements in Estonia, which ranged from 1 to 6 ppbv. For the highly time-resolved measurements we used hydrocarbon-like organic aerosol (HOA) multiplied by an NH_3/HOA factor determined in Elser *et al.* (2018) instead of NH_3.[15] Elser *et al.* showed that NH_3 time-series were averaged out with slower response times due to the stickiness of the molecule, and HOA was shown to be the best traffic tracer. We identified two different "spike" variations from the data: frequent small spikes of up to 2 ppbv increase in NH_3 for approximately two minutes every 15 minutes, and less frequent intense spikes of at least 10 ppbv for approximately three minutes every 25 minutes. These values were used in the simulations of NH_3 inhomogeneities. The background ammonia concentration used in the simulations was 1 ppbv. This is a low estimation for background ammonia in cities, but it allows for exploring the effect of small and large perturbations in the concentration.

3 Results

3.1 Model validation at −10 °C using CLOUD chamber data

Experiments involving growth from ammonium nitrate formation were undertaken at 20 °C, 5 °C and −10 °C in the CLOUD chamber at CERN. The experiments were designed to use atmospherically relevant concentrations of all gases. Fig. 1a shows

results from all of the CLOUD experiments as triangular points where the newly formed particles were activated by ammonium nitrate formation. We observe ammonium nitrate growth at 5 °C and −10 °C but not at 20 °C at the concentrations used in our study. At the lower temperature, lower gas-phase concentrations can result in higher growth rates. This is partially due to the fact that the saturation concentration of ammonium nitrate is lower at lower temperatures and therefore more NH_3 and HNO_3 can condense. Plotted with this data, as diamond points, are the growth rates obtained from model simulations with constrained gas phase concentrations of HNO_3 and NH_3 from CLOUD measurements. We use MCM[21,22] to model the chemistry in the chamber, using measured gas-phase time-series, measured loss rates of vapours, and photolysis rates from CLOUD.

The measured and modelled growth rates are plotted against the limiting gas for ammonium nitrate formation, which is either NH_3 or HNO_3. The limiting gas determines the amount of NH_4NO_3 that can condense on particles, thus the growth rate increases with increasing concentration. However, this relationship is not strictly linear as the growth also depends on which gas is limiting condensation (see Marten *et al.* (2022)[13] ESI† for full explanation); it is used here only to display the data. Fig. 1b directly compares the measured CLOUD growth rates and model growth rates shown in Fig. 1a, a dashed line of $x = y$ is also shown. From these two plots, it is clear that the kinetic model is capable of replicating CLOUD results not only at 5 °C but also at −10 °C.
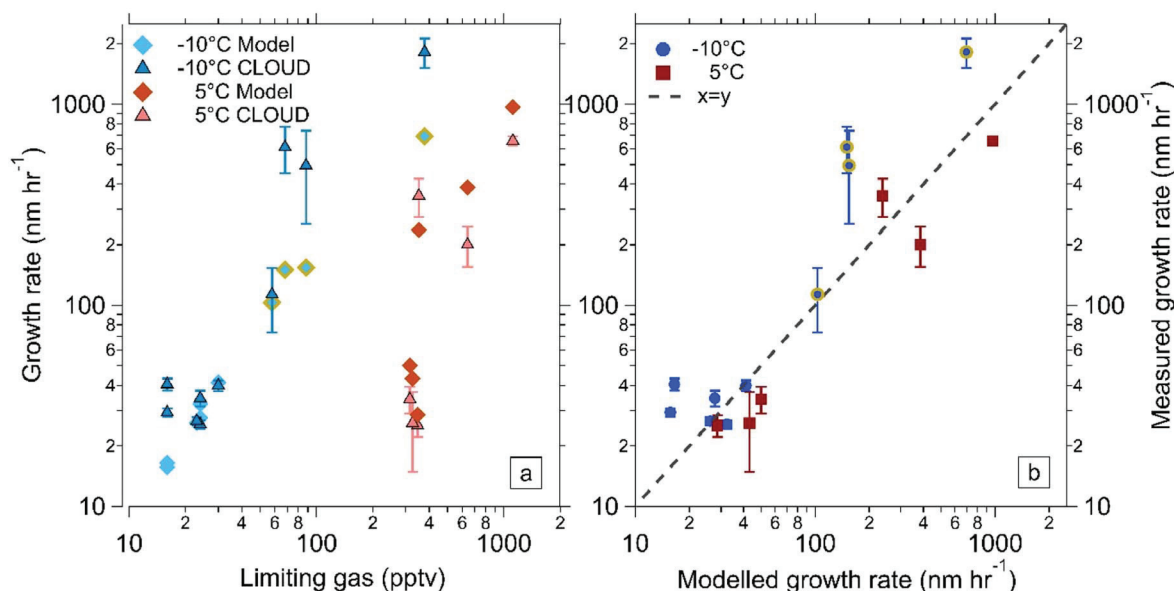

Fig. 1 Comparison of measured and modelled growth rates at 5 °C and −10 °C. (a) Measured (triangles with error bars) and modelled (diamonds) growth rates at 5 °C and −10 °C, 60% RH, *versus* the limiting gas for ammonium nitrate condensation, which is either ammonia or nitric acid and is experiment dependent. The CLOUD measured growth rates were determined using the 50% appearance time method.[26] The modelled data points were determined using the same method on output from the kinetic model, constrained by measured gas–phase concentrations from CLOUD experiments. The modelled values at −10 °C also included modelled N_2O_5 concentrations which may have contributed to growth, those with a thick golden border had 10 s to 100 s of pptv of N_2O_5. All measured data points and modelled data points at 5 °C were previously presented in Wang *et al.* (2020)[12] and Marten *et al.* (2022).[13] (b) Modelled growth rates *versus* measured growth rates at 5 °C and −10 °C for all the experiments shown in (a).

For the points indicated in Fig. 1a at $-10\,^{\circ}$C by a thick golden border, we calculated that there were tens to hundreds of pptv of N_2O_5. Due to differing chemistries, the remaining experiments had negligible N_2O_5 concentration (Table S1†). Original model results using HNO_3 concentrations alone (Fig. S1†) resulted in some simulations with growth rates that were much lower than the experimental results. The results were parameterised for N_2O_5 uptake by including additional HNO_3, which resulted in better agreement between the experiment and model results. The uptake of N_2O_5 into small ammonium nitrate particles is not well characterized. Uptake rates determined from ambient measurements are approximately a few percent, but strongly increase with the aerosol water content. Without N_2O_5 measurements, modelling the condensation flux of N_2O_5 is subject to substantial uncertainties, because (1) the uptake rate coefficient of N_2O_5 onto small ammonium nitrate particles has not been previously determined, and (2) the wall loss behaviour of N_2O_5 in the CLOUD chamber is unknown. For our modelled values, we considered a kinetic condensation of the N_2O_5 as an upper limit and a complete loss of N_2O_5 onto the walls, which would yield a lowest estimate of N_2O_5 concentrations, which may explain why the growth rates are still underpredicted. N_2O_5 concentrations calculated without wall loss are also significantly higher and are shown in Table S1.† Under these assumptions, model to measurement discrepancy decreases from a factor of 10 to factor of 2.5. We concluded, albeit with uncertainty, that N_2O_5 may be a missing gas contributor to growth, but more experiments would be needed to measure the N_2O_5 uptake rates as a function of particle size and chemical composition.

3.2 Effect of temperature change during vertical transport

Using our experimentally validated model, we explored the effect of the changing temperature of a rising air parcel in a city on the overall size distribution. In these experiments, we also include an initial particle size distribution, which is lognormal and centred around 200 nm, in order to simulate a condensation sink of $0.005\ \text{s}^{-1}$. Fig. 2 shows the size distribution *versus* time of an air parcel with constant temperature (Fig. 2a), an air parcel with several decreases and subsequent increases in temperature (Fig. 2c) and the respective temperature profiles plotted in Fig. 2b. The activation diameter (d_{act}) is defined as the critical size at which ammonium nitrate can condense on particles and is dependent on the temperature, gas phase concentrations of NH_3 and HNO_3, and the Kelvin diameter. d_{act} is plotted as a black line in both Fig. 2a and c. During each temperature drop the activation diameter decreases, and particles as small as 5 nm can rapidly grow from ammonium nitrate formation. The largest newly formed particles start to rapidly grow from less than 10 nm to around 50 nm. When the temperature increases as the air parcel returns to ground level, part of the NH_4NO_3 evaporates, resulting in a slight shrinking in the size distribution of the original condensation sink and the newly growing particles. However, this shrinkage does not result in a complete re-evaporation of the new particles and the net effect of the temperature change is the formation of new

Aitken mode particles. Fig. 2d shows the size distributions at the end of the experiments with and without a change in temperature, and a control experiment for each, with the same condensation sink and temperature profiles but without new particle formation. In the case of constant temperature, there are two distinct modes, with a minimum particle concentration around 20 nm, *i.e.* the size that the new particles were able to grow to. By contrast, in the experiment with changing temperature the lower mode has grown as high as 50 nm and has considerably larger particle number concentrations. These results show that vertical mixing in a typical urban environment can stimulate growth from ammonium nitrate formation. This may help to increase the particle number of larger sizes and aid in survival of newly formed particles through the valley of death, even after returning to surface temperature and sub-saturated conditions. We acknowledge that this is a simplistic model and in reality, a decrease in temperature will also result in an increase in relative humidity and deliquescence of particles. If the effect of water were taken into account, the dissociation constant would be affected by the change of state and most likely result in more condensation of ammonium nitrate, therefore resulting in a larger effect on the particle size distribution than simulated here.

We assessed the conditions required for ammonium nitrate to activate nucleated particles through sensitivity tests. We observed that a larger and faster temperature change results in more pronounced activation (Fig. S2 and S3†). At lower nucleation rates the effect of ammonium nitrate on growth is lessened, since fewer particles are present for activation (Fig. S4†). We also show that higher initial temperatures will result in a much larger change in supersaturated ammonia and nitric acid concentrations, which will be available for rapid particle growth (Fig. S5 and S6†). Therefore, the occurrence of this process requires sufficient pre-existing particles above the activation diameter and sufficient ammonium nitrate concentration above the saturation concentration. Such conditions are promoted by higher nucleation rates, higher boundary layer temperatures, and higher and faster changes in temperature.

3.3 Effect of inhomogeneity of NH_3 concentrations in cities

In typical urban environments air parcels will experience temporal inhomogeneities in gas-phase concentrations in addition to vertical mixing. Therefore, we set up a simulation with a variable ammonia time-series, meant to represent an area close to a source with large, sporadic variations in ammonia, such as traffic.[15] We also include the same initial particle size distribution as in Fig. 2. Fig. 3a shows an experiment with fixed production rates of HNO_3, NH_3, and H_2SO_4, where newly formed particles have grown to ~20 nm by the end of the simulation. The production values of NH_3, HNO_3, and H_2SO_4 were calculated such that in the absence of condensation, the concentrations were 1 ppbv, 0.2 ppbv, and 1×10^7 molecules per cm^3 respectively. The concentrations were chosen as typical background concentrations, resulting in an activation diameter of 200 nm for ammonium nitrate growth. In Fig. 3c the simulation in Fig. 3(a) is repeated but with a variable

© 2024 The Author(s). Published by the Royal Society of Chemistry

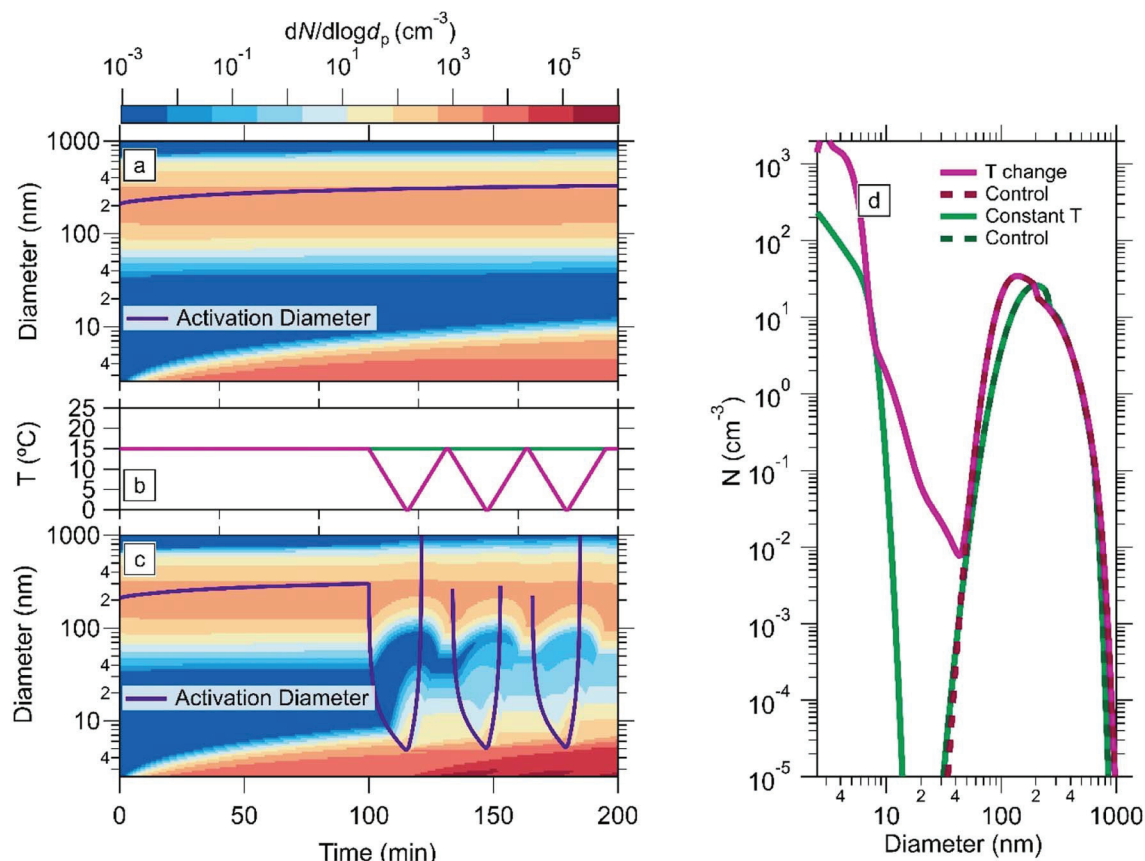*Environ. Sci.: Atmos.*, 2024, **4**, 265–274 | **269**

Fig. 2 Model simulation of a temperature change in an air parcel due to vertical transport. (a) Size distribution of an experiment with constant temperature with an indigo trace showing d_{act}. Initial conditions are 3 ppbv NH_3, 1 ppbv HNO_3 and 1×10^7 molecules per cm^3 H_2SO_4. (b) Temperature profiles for constant temperature (green) and with temperature change (magenta). (c) Size distribution of an experiment with a temperature change simulating an air parcel moving up and down with an indigo curve showing d_{act}. Initial conditions are the same as in (a). (d) Particle size distributions at the end of (a) (green) and (c) (magenta). The experiment with the temperature change has a large increase in particles up to around 50 nm, where the newly formed particles have grown to, whereas when there is no temperature change the newly formed particles have only grown to around 10 nm.

NH_3 time-series, with alternate "spikes" of 10 ppbv and 2 ppbv and a background concentration of 1 ppbv. The NH_3 time-series is presented in Fig. 3(b). We observe that the newly formed particles have grown much larger than in Fig. 3(a), reaching the size of the original condensation sink. The concentration of particles above 50 nm, represented by black diamonds in Fig. 3(a) and (c), increases in Fig. 3(c) as new particles grow, whereas it slowly but steadily decreases in Fig. 3(a). Fig. 3d shows the size distributions corresponding to the first and last diamond points in Fig. 3(a) and (c). The blue trace, representing the final diamond in Fig. 3(a), differs from the starting size distribution with the appearance of the nucleation mode up to around 20 nm and by growth of the largest particles as the second mode shifts right. In addition to these changes, the orange trace, which represents the end diamond in Fig. 3(c), has dramatically increased particle number concentration up to 200 nm. From this we conclude that inhomogeneities in NH_3 emissions can sustain particle number by causing temporary supersaturation of ammonium nitrate, and growing particles through the valley of death.

In all of the simulations presented, we also model the particle composition throughout. Fig. S7† shows examples of plots with the relative concentrations of ammonium nitrate and ammonium sulfate. These results show that the fraction of NH_4NO_3 is only significant during the supersaturated periods and above the activation diameter. Once sub-saturated conditions resume, the ammonium nitrate quickly evaporates. However, Fig. 2 and 3 show that even after NH_4NO_3 evaporates into gas phase NH_3 and HNO_3, the edge of the growing particle size distribution still survives at larger sizes than before activation. This is because NH_4NO_3 condensation, even if it is brief and reversible, increases the survival rate of newly formed particles, making them less susceptible to coagulation loss.

4 Discussion and conclusions

In light of these results, it may be puzzling that similar size distributions as in Fig. 3 have not been frequently observed in ambient measurements. Experiments in the CLOUD chamber involved supersaturated conditions of ammonia and nitric acid, resulting in rapid particle growth, allowing the chemistry and
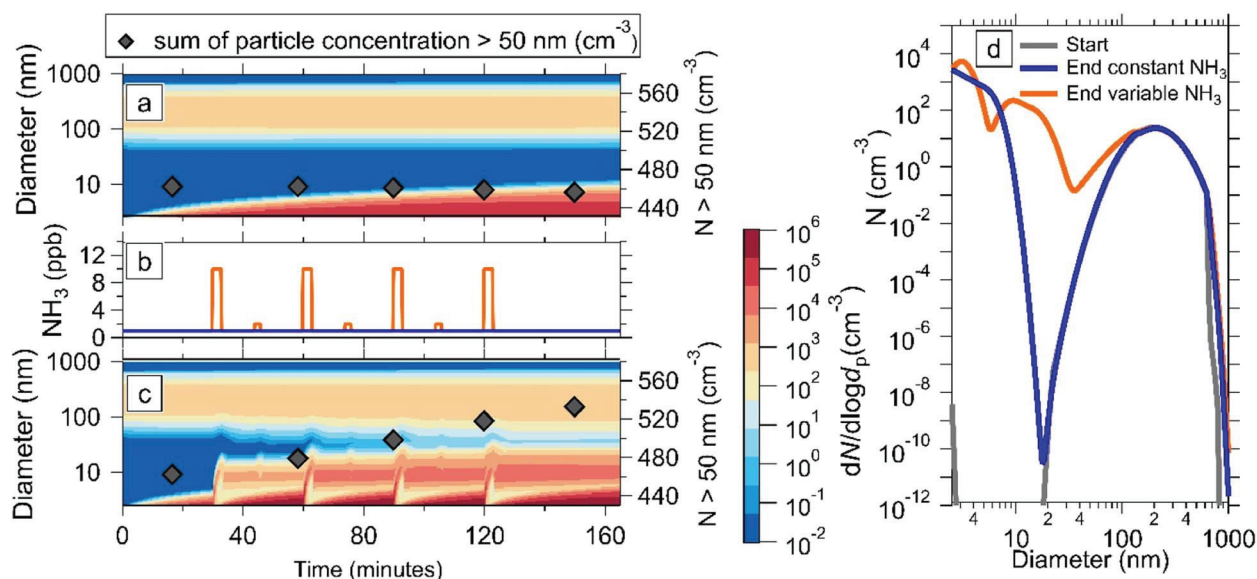
Fig. 3 Model simulation of inhomogeneities in the NH_3 time-series. (a) Model simulation at 5 °C with constant production rates of NH_3 and HNO_3 with sum of all particles above 50 nm scattered in diamond points which are steadily decreasing. Initial concentrations are 1 ppbv NH_3, 0.2 ppbv HNO_3, and 1×10^7 molecules per cm^3 H_2SO_4. (b) Gas phase concentrations of NH_3 from (a) (blue) and (c) (orange). (c) Model experiment at 5 °C with alternating 10 ppbv and 2 ppbv high 'spikes' of NH_3 concentration with duration of three and two minutes, respectively, simulating inhomogeneity. Initial conditions are the same as in (a). The sum of all particles above 50 nm is scattered in diamond points and is steadily increasing. The particle concentration is plotted before a new inhomogeneity started, when the model was in steady state. (d) Particle size distributions at the start and end of (a) and (c).

particle microphysics of ammonium nitrate growth in the nanoparticle range to be verified. In the real atmosphere ammonium nitrate will mostly be found in equilibrium with its gas-phase counterparts, resulting in no particle growth. The model was therefore designed to simulate ambient atmospheric scenarios that would result in a short perturbation of equilibrium. We observe that in these conditions of high heterogeneities, although short-lived, rapid growth due to ammonium nitrate formation can occur.

To the best of our knowledge, the rapid particle growth from ammonium nitrate formation has not been previously reported. One of the many reasons for the lack of ambient observations of this phenomenon could be the low resolution of particle size distribution measurements. Fig. S8† shows the same size distribution as in Fig. 3c, but with a lower time resolution of 5 minutes, and a diameter resolution and range of a typical scanning mobility particle sizer. The features are not as distinguished as those presented from the model results. In the simulations presented in Fig. 3c the inhomogeneities lasted only 2–3 minutes, which would be challenging to capture on an instrument with a 5 minutes resolution. This results in less obvious changes in the size distribution, with some features that could be interpreted as noise. In addition, more than one particle sizing instrument would be required to measure the diameter range and resolution presented from model results. Furthermore, at sustained concentrations of NH_4NO_3 in the absence of inhomogeneities, equilibrium is rapidly reached, and the required supersaturation for rapid growth is no longer present. Finally, these measurements would need to take place

near to a large source of NH_3 or HNO_3, such as traffic, and background sites would therefore not measure such distributions. Additionally, direct particle emissions also result in pulses of primary particles, especially with high time resolution measurements, further blurring the interpretation of new particle formation events. The effect of the condensation sink on particle survival was presented in Marten *et al.* (2022) and revealed that even under condensation sinks over 0.01 s^{-1} [NH_3] × [HNO_3] concentrations higher than 1.2 ppb^2 led to survival rates close to unity.[13] In the experiments simulated in this paper, [NH_3] × [HNO_3] values were around 4 ppb^2, which means that particle survival is relatively independent of the condensation sink. To summarise, although it is likely that this mechanism may occur in urban ambient air, it is hard to identify and it needs specific conditions with high heterogeneity coming from either large differences in temperatures or large emissions of ammonia (>10 ppbv).

It is important to point out that this model does not take into account the effect of relative humidity on the ammonium nitrate system. Since all of the experiments were performed with a relative humidity lower than the deliquescence relative humidity (DRH) of ammonium nitrate (62% at 25 °C, and higher at lower temperatures[2]), it might be considered a solid. However, as the efflorescence of NH_4NO_3 is below 40% (ref. 27) and since atmospheric aerosols are typically multicomponent in nature, it is likely that under most conditions, at least a fraction of NH_4NO_3 will be present in an aqueous solution. Although in the conditions presented in this paper water most likely does not affect ammonium nitrate growth, there are other

© 2024 The Author(s). Published by the Royal Society of Chemistry

Environ. Sci.: Atmos., 2024, **4**, 265–274 | **271**

conditions where water may play a larger role. Ambient, wet, conditions are even more likely to be supersaturated than corresponding dry conditions. Due to the Kelvin effect, water is less likely to condense on smaller particles, and therefore small particles will tend to contain less water than larger particles. Ammonium nitrate ionic strength also affects the dissociation constant, where K_p decreases with increasing ionic strength. In summary, larger particles in wet conditions will be liquid, and since this affects the dissociation constant, more ammonium nitrate should be able to condense on particles and increase the effect of NH_4NO_3 growth on the particle size distribution. This effect should be verified with further chamber experiments at higher relative humidity.

Our results highlight additional gaps in understanding the effect of temperature changes and inhomogeneous emissions on particle growth. At -10 °C, calculated N_2O_5 concentrations correlated with a growth rate enhancement in 4 out of 10 experiments. Whether N_2O_5 is the cause of this enhancement could not be corroborated experimentally, and warrants further investigation, especially for sub-10 nm particles. Changes in temperature will also have additional effects on nucleation and growth from other vapours in urban atmospheres. For example, anthropogenic low-volatility organic compounds (LVOCs) may increasingly condense at lower temperatures, which has not yet been fully assessed experimentally. Finally, future experimental and modelling studies should take the effect of relative humidity and water uptake on the condensation of ammonium nitrate into account.

We have shown that rapid particle growth through ammonium nitrate formation requires a large and rapid change in temperature, a sufficient pre-existing particle distribution, and high enough gas-phase concentrations of NH_3 and HNO_3. In the absence of a temperature change, inhomogeneous emissions of ammonia can also cause rapid growth. This phenomenon could occur close to emission sources, but observation would require high time- and size-resolved particle measurements. It is possible that such phenomena have not been observed due to factors such as location and time or diameter resolution.

Author contributions

Conceptualization: R. M., M. X., M. W., J. Dommen, J. K., N. M. D., H. L., U. B. and I. E. H., resources, prepared the CLOUD facility or measuring instruments: R. M., M. W., W. K., X.-C. H., D. S., J. P., G. M., D. S. W., A. B., C. P. L., A. A., D. M. B., R. B., L. C., L. D., J. Duplissy, H. F., M. H., K. L., H. E. M., B. M., T. P., M. P., B. R., W. S., J. S., Y. J. T., A. T., A. C. W., S. K. W., M. Z.-W., J. K., H. L., and I. E. H. Investigation: R. M., M. X., M. W., W. K., X.-C. H., D. S., J. P., G. M., D. S. W., A. B., C. P. L., R. B., D. M. B., B. B., L. C., L. D., J. Duplissy, H. F., M. H., M. L., H. E. M, B. M., W. S., J. S., Y. J. T., A. C. W., S. K. W., M. Z.-W., J. K., H. L., and I. E. H. Formal analysis: R. M., M. W., W. K., X. H., D. S., J. P., G. M., D. S. W., S. K. W., H. L., and I. E. H. Scientific discussion: R. M., M. X., M. W., W. K., X.-C. H., D. S., D. B., L. D., K. L., J. Dommen, R. C. F., J. K., N. M. D., H. L., U. B., and I. E. H. Writing: R. M., M. W., W. K., X.-C. H., D. S., J. Dommen, J. K., N. M. D., H. L., U. B., and I. E. H.

Conflicts of interest

There are no conflicts to declare.

Acknowledgements

References

1 T. F. Stocker, D. Qin, G.-K. Plattner, M. Tignor, S. K. Allen, J. Boschung, A. Nauels, Y. Xia, V. Bex and P. M. Midgeley, *Climate Change 2013 The Physical Science Basis*, Intergovernmental Panel on Climate Change (IPCC), 2013.

2 J. H. Seinfeld and S. N. Pandis, *Atmospheric Chemistry and Physics*, John Wiley & Sons, 2nd edn, 2006.

3 WHO, *Methods and Data Sources for Country-Level Causes of Death 2000-2019*, World Health Organisation, 2020.

4 WHO, *Methods and Data Sources for Global Burden of Disease Estimates 2000-2019*, World Health Organisation, 2020.

5 L. Yao, O. Garmash, F. Bianchi, J. Zheng, C. Yan, J. Kontkanen, H. Junninen, S. B. Mazon, M. Ehn, P. Paasonen, M. Sipilä, M. Wang, X. Wang, S. Xiao, H. Chen, Y. Lu, B. Zhang, D. Wang, Q. Fu, F. Geng, L. Li, H. Wang, L. Qiao, X. Yang, J. Chen, V.-M. Kerminen, T. Petäjä, D. R. Worsnop, M. Kulmala and L. Wang, Atmospheric new particle formation from sulfuric acid and amines in a Chinese megacity, *Science*, 2018, **361**, 278–281.

6 S. Xiao, M. Y. Wang, L. Yao, M. Kulmala, B. Zhou, X. Yang, J. M. Chen, D. F. Wang, Q. Y. Fu, D. R. Worsnop and L. Wang, Strong atmospheric new particle formation in winter in urban Shanghai, China, *Atmos. Chem. Phys.*, 2015, **15**, 1769–1781.

7 Z. B. Wang, M. Hu, J. Y. Sun, Z. J. Wu, D. L. Yue, X. J. Shen, Y. M. Zhang, X. Y. Pei, Y. F. Cheng and A. Wiedensohler, Characteristics of regional new particle formation in urban and regional background environments in the North China Plain, *Atmos. Chem. Phys.*, 2013, **13**, 12495–12506.

8 D. Bousiotis, M. Dall'Osto, D. C. S. Beddows, F. D. Pope and R. M. Harrison, Analysis of new particle formation (NPF) events at nearby rural, urban background and urban roadside sites, *Atmos. Chem. Phys.*, 2019, **19**, 5679–5694.

9 Z. Wang, Z. Wu, D. Yue, D. Shang, S. Guo, J. Sun, A. Ding, L. Wang, J. Jiang, H. Guo, J. Gao, H. C. Cheung, L. Morawska, M. Keywood and M. Hu, New particle formation in China: Current knowledge and further directions, *Sci. Total Environ.*, 2017, **577**, 258–266.

10 V.-M. Kerminen and M. Kulmala, Analytical formulae connecting the "real" and the "apparent" nucleation rate and the nuclei number concentration for atmospheric nucleation events, *J. Aerosol Sci.*, 2002, **33**, 609–622.

11 M. Xiao, C. R. Hoyle, L. Dada, D. Stolzenburg, A. Kürten, M. Wang, H. Lamkaddam, O. Garmash, B. Mentler, U. Molteni, A. Baccarini, M. Simon, X.-C. He, K. Lehtipalo, L. R. Ahonen, R. Baalbaki, P. S. Bauer, L. Beck, D. Bell, F. Bianchi, S. Brilke, D. Chen, R. Chiu, A. Dias, J. Duplissy, H. Finkenzeller, H. Gordon, V. Hofbauer, C. Kim, T. K. Koenig, J. Lampilahti, C. P. Lee, Z. Li, H. Mai, V. Makhmutov, H. E. Manninen, R. Marten, S. Mathot, R. L. Mauldin, W. Nie, A. Onnela, E. Partoll, T. Petäjä, J. Pfeifer, V. Pospisilova, L. L. J. Quéléver, M. Rissanen, S. Schobesberger, S. Schuchmann, Y. Stozhkov, C. Tauber, Y. J. Tham, A. Tomé, M. Vazquez-Pufleau, A. C. Wagner, R. Wagner, Y. Wang, L. Weitz, D. Wimmer, Y. Wu, C. Yan, P. Ye, Q. Ye, Q. Zha, X. Zhou, A. Amorim, K. Carslaw, J. Curtius, A. Hansel, R. Volkamer, P. M. Winkler, R. C. Flagan, M. Kulmala, D. R. Worsnop, J. Kirkby, N. M. Donahue, U. Baltensperger, I. El Haddad and J. Dommen, The driving factors of new particle formation and growth in the polluted boundary layer, *Atmos. Chem. Phys.*, 2021, **21**, 14275–14291.

12 M. Wang, W. Kong, R. Marten, X.-C. He, D. Chen, J. Pfeifer, A. Heitto, J. Kontkanen, L. Dada, A. Kürten, T. Yli-Juuti, H. E. Manninen, S. Amanatidis, A. Amorim, R. Baalbaki, A. Baccarini, D. M. Bell, B. Bertozzi, S. Bräkling, S. Brilke, L. C. Murillo, R. Chiu, B. Chu, L.-P. De Menezes, J. Duplissy, H. Finkenzeller, L. G. Carracedo, M. Granzin, R. Guida, A. Hansel, V. Hofbauer, J. Krechmer, K. Lehtipalo, H. Lamkaddam, M. Lampimäki, C. P. Lee, V. Makhmutov, G. Marie, S. Mathot, R. L. Mauldin, B. Mentler, T. Müller, A. Onnela, E. Partoll, T. Petäjä, M. Philippov, V. Pospisilova, A. Ranjithkumar, M. Rissanen, B. Rörup, W. Scholz, J. Shen, M. Simon, M. Sipilä, G. Steiner, D. Stolzenburg, Y. J. Tham, A. Tomé, A. C. Wagner, D. S. Wang, Y. Wang, S. K. Weber,

P. M. Winkler, P. J. Wlasits, Y. Wu, M. Xiao, Q. Ye, M. Zauner-Wieczorek, X. Zhou, R. Volkamer, I. Riipinen, J. Dommen, J. Curtius, U. Baltensperger, M. Kulmala, D. R. Worsnop, J. Kirkby, J. H. Seinfeld, I. El-Haddad, R. C. Flagan and N. M. Donahue, Rapid growth of new atmospheric particles by nitric acid and ammonia condensation, *Nature*, 2020, **581**, 184–189.

13 R. Marten, M. Xiao, B. Rörup, M. Wang, W. Kong, X.-C. He, D. Stolzenburg, J. Pfeifer, G. Marie, D. S. Wang, W. Scholz, A. Baccarini, C. P. Lee, A. Amorim, R. Baalbaki, D. M. Bell, B. Bertozzi, L. Caudillo, B. Chu, L. Dada, J. Duplissy, H. Finkenzeller, L. G. Carracedo, M. Granzin, A. Hansel, M. Heinritzi, V. Hofbauer, D. Kemppainen, A. Kürten, M. Lampimäki, K. Lehtipalo, V. Makhmutov, H. E. Manninen, B. Mentler, T. Petäjä, M. Philippov, J. Shen, M. Simon, Y. Stozhkov, A. Tomé, A. C. Wagner, Y. Wang, S. K. Weber, Y. Wu, M. Zauner-Wieczorek, J. Curtius, M. Kulmala, O. Möhler, R. Volkamer, P. M. Winkler, D. R. Worsnop, J. Dommen, R. C. Flagan, J. Kirkby, N. M. Donahue, H. Lamkaddam, U. Baltensperger and I. El Haddad, Survival of newly formed particles in haze conditions, *Environ. Sci.: Atmos.*, 2022, **2**, 491–499.

14 K. Lu, H. Fuchs, A. Hofzumahaus, Z. Tan, H. Wang, L. Zhang, S. H. Schmitt, F. Rohrer, B. Bohn, S. Broch, H. Dong, G. I. Gkatzelis, T. Hohaus, F. Holland, X. Li, Y. Liu, Y. Liu, X. Ma, A. Novelli, P. Schlag, M. Shao, Y. Wu, Z. Wu, L. Zeng, M. Hu, A. Kiendler-Scharr, A. Wahner and Y. Zhang, Fast Photochemistry in Wintertime Haze: Consequences for Pollution Mitigation Strategies, *Environ. Sci. Technol.*, 2019, **53**, 10676–10684.

15 M. Elser, I. El-Haddad, M. Maasikmets, C. Bozzetti, R. Wolf, G. Ciarelli, J. G. Slowik, R. Richter, E. Teinemaa, C. Hüglin, U. Baltensperger and A. S. H. Prévôt, High contributions of vehicular emissions to ammonia in three European cities derived from mobile measurements, *Atmos. Environ.*, 2018, **175**, 210–220.

16 J. Kirkby, J. Curtius, J. Almeida, E. Dunne, J. Duplissy, S. Ehrhart, A. Franchin, S. Gagné, L. Ickes, A. Kürten, A. Kupc, A. Metzger, F. Riccobono, L. Rondo, S. Schobesberger, G. Tsagkogeorgas, D. Wimmer, A. Amorim, F. Bianchi, M. Breitenlechner, A. David, J. Dommen, A. Downard, M. Ehn, R. C. Flagan, S. Haider, A. Hansel, D. Hauser, W. Jud, H. Junninen, F. Kreissl, A. Kvashin, A. Laaksonen, K. Lehtipalo, J. Lima, E. R. Lovejoy, V. Makhmutov, S. Mathot, J. Mikkilä, P. Minginette, S. Mogo, T. Nieminen, A. Onnela, P. Pereira, T. Petäjä, R. Schnitzhofer, J. H. Seinfeld, M. Sipilä, Y. Stozhkov, F. Stratmann, A. Tomé, J. Vanhanen, Y. Viisanen, A. Vrtala, P. E. Wagner, H. Walther, E. Weingartner, H. Wex, P. M. Winkler, K. S. Carslaw, D. R. Worsnop, U. Baltensperger and M. Kulmala, Role of sulphuric acid, ammonia and galactic cosmic rays in atmospheric aerosol nucleation, *Nature*, 2011, **476**, 429–433.

17 J. Duplissy, J. Merikanto, A. Franchin, G. Tsagkogeorgas, J. Kangasluoma, D. Wimmer, H. Vuollekoski, S. Schobesberger, K. Lehtipalo, R. C. Flagan, D. Brus,

© 2024 The Author(s). Published by the Royal Society of Chemistry

Environ. Sci.: Atmos., 2024, **4**, 265–274 | 273

N. M. Donahue, H. Vehkamäki, J. Almeida, A. Amorim, P. Barmet, F. Bianchi, M. Breitenlechner, E. M. Dunne, R. Guida, H. Henschel, H. Junninen, J. Kirkby, A. Kürten, A. Kupc, A. Määttänen, V. Makhmutov, S. Mathot, T. Nieminen, A. Onnela, A. P. Praplan, F. Riccobono, L. Rondo, G. Steiner, A. Tome, H. Walther, U. Baltensperger, K. S. Carslaw, J. Dommen, A. Hansel, T. Petäjä, M. Sipilä, F. Stratmann, A. Vrtala, P. E. Wagner, D. R. Worsnop, J. Curtius and M. Kulmala, Effect of ions on sulfuric acid-water binary particle formation: 2. experimental data and comparison with QC-normalized classical nucleation theory, *J. Geophys. Res.: Atmos.*, 2016, **121**, 1752–1775.

18 J. Voigtländer, J. Duplissy, L. Rondo, A. Kürten and F. Stratmann, Numerical simulations of mixing conditions and aerosol dynamics in the CERN CLOUD chamber, *Atmos. Chem. Phys.*, 2012, **12**, 2205–2214.

19 M. Mozurkewich, The dissociation constant of ammonium nitrate and its dependence on temperature, relative humidity and particle size, *Atmos. Environ., Part A*, 1993, **27**, 261–270.

20 A. C. K. Lai and W. W. Nazaroff, Modeling indoor particle deposition from turbulent flow onto smooth surfaces, *J. Aerosol Sci.*, 2000, **31**, 463–476.

21 C. Bloss, V. Wagner, M. E. Jenkin, R. Volkamer, W. J. Bloss, J. D. Lee, D. E. Heard, K. Wirtz, M. Martin-Reviejo, G. Rea, J. C. Wenger and M. J. Pilling, Development of a detailed chemical mechanism (MCM v3.1) for the atmospheric oxidation of aromatic hydrocarbons, *Atmos. Chem. Phys.*, 2005, **24**(5), 641–664.

22 M. E. Jenkin, S. M. Saunders, V. Wagner and M. J. Pilling, Protocol for the development of the Master Chemical Mechanism, MCM v3 (Part B): tropospheric degradation of aromatic volatile organic compounds, *Atmos. Chem. Phys.*, 2003, **3**(1), 181–193.

23 R. San Jose, F. J. Moreno and M. A. San Feliu, Field study on O_3, SO_2 and NH_3 deposition over a suburban area: Madrid case study, *Air Pollution and Visibility Measurements*, Proc. SPIE, 1995, vol 2506, pp. 274–285.

24 H. Gordon, J. Kirkby, U. Baltensperger, F. Bianchi, M. Breitenlechner, J. Curtius, A. Dias, J. Dommen, N. M. Donahue, E. M. Dunne, J. Duplissy, S. Ehrhart, R. C. Flagan, C. Frege, C. Fuchs, A. Hansel, C. R. Hoyle, M. Kulmala, A. Kürten, K. Lehtipalo, V. Makhmutov, U. Molteni, M. P. Rissanen, Y. Stozkhov, J. Tröstl, G. Tsagkogeorgas, R. Wagner, C. Williamson, D. Wimmer, P. M. Winkler, C. Yan and K. S. Carslaw, Causes and importance of new particle formation in the present-day and preindustrial atmospheres, *J. Geophys. Res.: Atmos.*, 2017, **122**, 8739–8760.

25 E. M. Dunne, H. Gordon, A. Kurten, J. Almeida, J. Duplissy, C. Williamson, I. K. Ortega, K. J. Pringle, A. Adamov, U. Baltensperger, P. Barmet, F. Benduhn, F. Bianchi, M. Breitenlechner, A. Clarke, J. Curtius, J. Dommen, N. M. Donahue, S. Ehrhart, R. C. Flagan, A. Franchin, R. Guida, J. Hakala, A. Hansel, M. Heinritzi, T. Jokinen, J. Kangasluoma, J. Kirkby, M. Kulmala, A. Kupc, M. J. Lawler, K. Lehtipalo, V. Makhmutov, G. Mann, S. Mathot, J. Merikanto, P. Miettinen, A. Nenes, A. Onnela, A. Rap, C. L. S. Reddington, F. Riccobono, N. A. D. Richards, M. P. Rissanen, L. Rondo, N. Sarnela, S. Schobesberger, K. Sengupta, M. Simon, M. Sipila, J. N. Smith, Y. Stozhkov, A. Tome, J. Trostl, P. E. Wagner, D. Wimmer, P. M. Winkler, D. R. Worsnop and K. S. Carslaw, Global atmospheric particle formation from CERN CLOUD measurements, *Science*, 2016, **354**, 1119–1124.

26 D. Stolzenburg, L. Fischer, A. L. Vogel, M. Heinritzi, M. Schervish, M. Simon, A. C. Wagner, L. Dada, L. R. Ahonen, A. Amorim, A. Baccarini, P. S. Bauer, B. Baumgartner, A. Bergen, F. Bianchi, M. Breitenlechner, S. Brilke, S. Buenrostro Mazon, D. Chen, A. Dias, D. C. Draper, J. Duplissy, I. El Haddad, H. Finkenzeller, C. Frege, C. Fuchs, O. Garmash, H. Gordon, X. He, J. Helm, V. Hofbauer, C. R. Hoyle, C. Kim, J. Kirkby, J. Kontkanen, A. Kürten, J. Lampilahti, M. Lawler, K. Lehtipalo, M. Leiminger, H. Mai, S. Mathot, B. Mentler, U. Molteni, W. Nie, T. Nieminen, J. B. Nowak, A. Ojdanic, A. Onnela, M. Passananti, T. Petäjä, L. L. J. Quéléver, M. P. Rissanen, N. Sarnela, S. Schallhart, C. Tauber, A. Tomé, R. Wagner, M. Wang, L. Weitz, D. Wimmer, M. Xiao, C. Yan, P. Ye, Q. Zha, U. Baltensperger, J. Curtius, J. Dommen, R. C. Flagan, M. Kulmala, J. N. Smith, D. R. Worsnop, A. Hansel, N. M. Donahue and P. M. Winkler, Rapid growth of organic aerosol nanoparticles over a wide tropospheric temperature range, *Proc. Natl. Acad. Sci. U.S.A.*, 2018, **115**, 9122–9127.

27 C. Peng, L. Chen and M. Tang, A database for deliquescence and efflorescence relative humidities of compounds with atmospheric relevance, *Fundam. Res.*, 2022, **2**, 578–587.